Peculiarities of an anomalous electronic current during atomic force microscopy assisted nanolithography on n-type silicon

Sergei F Lyuksyutov[1]**, Pavel B Paramonov, Ivan Dolog and Robert M Ralich**

Department of Physics, Buchtel College of Arts and Sciences, The University of Akron, Akron, OH 44325, USA

E-mail: sfl@physics.uakron.edu

Abstract

We report the observation of anomalously high currents of up to 500 μA during direct oxide nanolithography on the surface of n-type silicon {100}. Conventional nanolithography on silicon with an atomic force microscope (AFM) normally involves currents of the order of 10^{-10}–10^{-7} A and is associated with ionic conduction within a water meniscus surrounding the tip. The anomalous current we observe is related to an electrical breakdown resulting in conduction dominated by electrons rather than ions. We discuss the electron source during the AFM-assisted nanolithography process, and the possibility of using this breakdown current for nanoscale parallel writing.

(Some figures in this article are in colour only in the electronic version)

The invention of the atomic force microscope (AFM) [1] has opened up challenging opportunities for the surface modification of metals, semiconductors and polymer materials. AFM-assisted surface oxidation (anodization) of semiconductors using electrically biased AFM tips [2, 3] is one of the techniques currently being considered for nanofabrication and nanoelectronics. In the past decade some progress in experimental AFM-assisted oxidation has been made in different areas including DC voltage AFM oxidation [3], non-contact AFM surface anodization [4], and AC voltage modulation techniques [5, 6]. Several examples of micro- and nanodevice fabrication using AFM lithography include side gate transistors [7], field effect transistors [8] in which amorphous silicon is patterned to fabricate a device [9], and waveguide division multiplexing [10]. The most impressive results include the fabrication of a conducting channel in aluminium consisting of a single atom [11].

Despite the variety of different AFM-assisted techniques, the physics of the electrochemical process and the behaviour of the electric current through the tip–sample interface are not understood completely. Most of the experimental evidence of SPM oxidation in semiconductors and metals presented so far indicates that ion transport is a rate-determining step in the oxidation process, related to the ionic current through the water meniscus during AFM-assisted lithography. It has been reported in [12], that strong electric field at bias voltages above 10 V, may inject 'hot' electrons into conduction band of silicon oxide, thus changing the process of SPM-oxidation resulting in 0.1–0.6 μA current. Our experimental study suggests that the anomalous current (up to 500 μA) is, in addition to its electronic nature, associated with water meniscus ionization. A major constraint on AFM-assisted oxidation is the speed of the process. An AFM tip writes one structure (line or a dot) at a time while moving (normally at speed 10–1000 μm s^{-1}) thus making the process serial, and therefore not scalable. The tip has to travel laterally miles in this serial process, and therefore it would require too long a time to fabricate a chip. This seriality of the process significantly limits AFM nanolithography capabilities, and brings to question its future as a nanotechnological tool.

In this work we report the experimental evidence of an anomalous electronic current during AFM-assisted silicon oxidation, which is not related to the Faradaic process associated with the ionic current. We obtain our results on n-type {100} and {111} silicon under ambient humidity. Special

[1] Author to whom any correspondence should be addressed.

attention is given to n-type Si {100} due to its importance in contemporary nanoelectronic technologies. A Digital Instruments Nanoscope II AFM modified in-house for the force–distance measurements was used in this study. K-TEK AFM tips of tip radius of 35 nm coated with a highly conductive W_2C film of thickness of 25 nm were used for surface anodization. Bias voltages in the range 0–50 V (negative) were applied to the AFM tip using an in-house built system. All experiments were conducted in a class 100 Clean Room under ambient humidity (normally 30–50%). The n-type Si {100}, and {111} substrates with the resistance 75–125 Ω cm^{-1} were cleaned in a 10 wt% hydrofluoric acid solution (HF:de-ionized water 1:5 by volume) for 2–3 min followed by rinsing with de-ionized water, and blowing under nitrogen before processing. Contact AFM imaging was performed to verify the absence of surface defects. The roughness of the surface after the surface passivation was less than 0.25 nm.

To monitor the current during AFM-assisted oxidation a Keithely 6485 picoammeter serially connected between the tip and negative bias or between the silicon wafer and ground was used. We observed an ionic current of the order 1–100 pA, associated with the transport of OH$^-$ ions. This current is related to the Faradaic process at the interface: anodic oxidation of the silicon surface occurs, and a nearly exponential current growth with respect to the applied voltage is observed. The current is presented in figure 1(a). The behaviour changes both qualitatively and quantitively between -20 and -30 V of the bias voltage. The electric current saturates at approximately 0.1 nA and then jumps dramatically several orders of magnitude. The threshold bias voltage at which the breakdown occurs depends on a number of experimental parameters such as the doping level of n-type silicon samples, tip–sample separation, the quality of surface termination, and the weariness of the AFM tip. We monitor anomalously high current in the range 100–500 μA for the bias voltages in the range -17 to -48 V. This current is presented in the figure 1(b) and is Ohmic. Line 1 in figure 1(b) represents the continuation of the curve shown in figure 1(a). Line 2 corresponds to electronic current measurements for low voltages taken after the breakdown has already occurred in order to verify the linearity of the i–V dependence. Line 3 corresponds to the measurements taken at a smaller tip–surface separation than that for line 2. Some overlap of the ionic and electronic currents indicates the existence of both types during the breakdown, although the electronic current is several orders of magnitude higher than the ionic one.

We also studied the formation of the dot structures during AFM-assisted oxidation. Analysis of the height and the volume of the dots at different bias voltages for the normal ionic current mode indicates that the growth of the dots is limited by a field-assisted diffusion process of hydroxyl ions (OH$^-$) through the layer of silicon oxide. At the point when oxidation is no longer assisted by the electric field the height and the logarithm of volume of the dots vary linearly with respect to the voltage. This is in good agreement with the Faradaic character of the observed I–V dependence (figure 1(a)), and similar behaviour has been reported for p-Si {100} in [13]. The self-limiting kinetics of oxide growth corresponds to temporal decay of the ionic current, presented in figure 2. The initial current (I_0) increases as the tip bias voltage increases. This
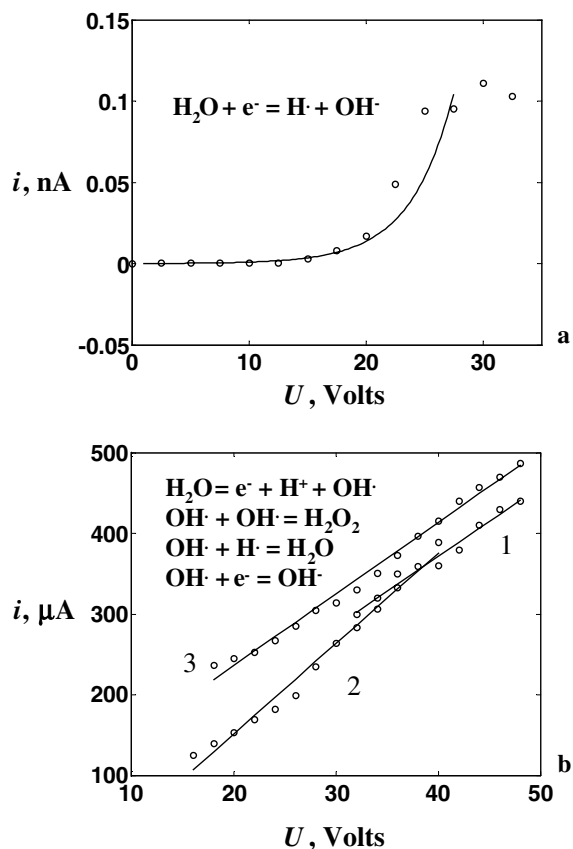

Figure 1. (a) The ionic current dependence on voltage for n-type H-terminated silicon 75–125 Ω cm^{-1}. Insert, the chemical reaction showing the yield of hydroxyl ions due to water reduction at the tip. (b) The electronic current dependence on voltage for n-type H-terminated silicon 75–125 Ω cm^{-1}. Curve 1, AFM tip in contact mode with undeflected cantilever ($V_{defl} = 0.0$ V); curve 2, same as curve 1, recorded after breakdown has already occurred in a particular spot; curve 3, the AFM tip is driven towards the surface ($V_{defl} = 2.5$ V). Insert, the chemical reaction for water ionization resulting in an electronic current.

current decreases rapidly with time as presented for curves at -5 V (1) and -9 V (2) bias voltages. This is not the case for breakdown current, if the bias voltage exceeds the threshold and the current jumps up several orders of magnitude: stable conductive channels are formed and almost no temporal decay of the current is observed, as shown in figure 2, curve 3 (-25 V).

We have performed multiple measurements of the force–distance curves during AFM-assisted nanolithography in a range of voltages below and above the breakdown. The size of approach–withdrawal hysteresis (Z-hysteresis), and the magnitude of the force are found to be very different with and without applied voltage. The general trend reveals an increase in the magnitude of the snap-off force and the size of the Z-hysteresis with voltage. The height of the water meniscus between the AFM tip and the silicon surface is reflected in the difference between the snap-on point without bias voltage and the snap-off point when the voltage is applied. We found it more accurate to redefine the Z-hysteresis as introduced in [13] through the difference of two hystereses: with and without an applied voltage to the AFM tip as (Z-$hyst$)$_V$ and (Z-$hyst$)$_0$, respectively. In this approach the Z-hysteresis without voltage
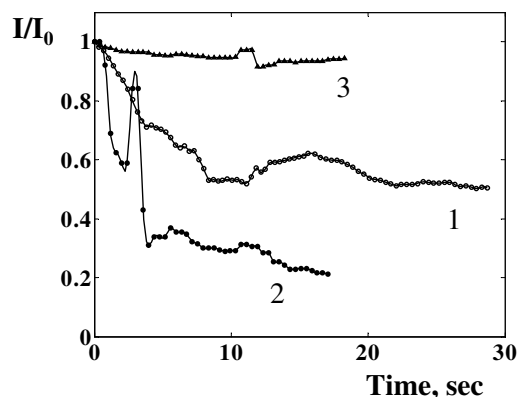
Figure 2. Temporal evolutions of a normalized current for different bias voltages: -5 V (curve 1), -9 V (curve 2), -25 V (curve 3), where I_0 is the initial current. Below breakdown (curves 1 and 2) the current decays in time suggesting an ionic SPM oxidation process, while at the breakdown regime the current is stable (curve 3).

$(Z\text{-}hyst)_0 = D_{off}^0 - D_{on}^0$ is used as a reference for the Z-hysteresis when voltage is applied $(Z\text{-}hyst)_V = D_{off}^V - D_{on}^V$, although the difference of the two indicates growth of the meniscus height with voltage: $(Z\text{-}hyst)_V - (Z\text{-}hyst)_0 = D_{off}^V - D_{on}^0$. Here, D_{on}^0, D_{off}^0 are the snap-on and off points with zero voltage and D_{on}^V, D_{off}^V are the same points when the voltage is applied. Figure 3(a) shows the force distance curves for two typical Z-hystereses above the breakdown ($U = -35$ V; curves 3, 4) and below ($U = -5$ V; curves 1, 2) the breakdown. The dependence of the Z-hysteresis with respect to the voltage is presented in figure 3(b). It is clearly seen that Z-hysteresis grows linearly with the bias voltage below and above the electrical breakdown indicating the growth of the water meniscus height and diameter. Analysis of the force distance dependences suggests that mainly two attractive forces: electrostatic and capillary play the major role in tip–surface interaction and increase with the bias voltage. This, in turn, results in an increase in the amount of water around the AFM tip related to electric field enhanced water condensation within the tip–sample area due to electrostatic attraction of polarized water molecules to the negatively charged AFM tip. The shape of the meniscus is dependent on the spatial distribution of the electric field at the end of the tip and the magnitude of the contact angle on the water–silicon interface. Presumably, the meniscus has the same shape for different voltage magnitudes, and grows linearly in lateral and vertical dimensions with respect to the bias voltage.

We study the formation of silicon oxide dots below and above the threshold voltage. A dot written below the breakdown is presented in figure 4(a). The diameter of the dot (50 nm) is comparable with the meniscus size, and the height of the dot (2.2 nm) is typical for AFM-assisted oxidation in silicon. When the voltage is at the threshold of the breakdown, a second oxide ring begins to form (figure 4(b)), grows in time, and is completely formed around an original spot as indicated in figure 4(c). The breakdown is always accompanied by the formation of the one or several rings around the original dot. We excluded the possibility that the rings are a result of material deposited from the tip. The AFM tips used in our study were coated with thermodynamically stable tungsten
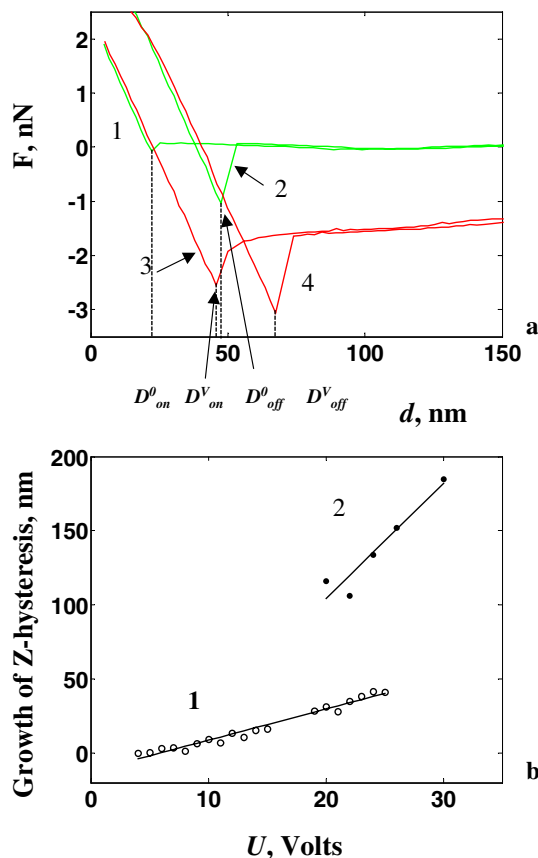

Figure 3. (a) Force–distance curves for two typical Z-hystereses. Curves 1 and 2, trace and retrace curves below breakdown, respectively; curves 3 and 4, trace and retrace above breakdown. (b) The growth of Z-hysteresis $(Z\text{-}hyst)_V - (Z\text{-}hyst)_0 = D_{off}^V - D_{on}^0$ with respect to the voltage. Here, D_{on}^0, D_{off}^0 are the snap-on and off points with zero voltage and D_{on}^V, D_{off}^V are the same points when the voltage is applied. Curve 1, below breakdown; curve 2, above breakdown. The force constant of the AFM cantilevers is between 0.1 and 0.9 N m^{-1}.

carbide (W$_2$C). Additionally, the volume estimate of the produced surface features significantly exceeds the amount of the tip coating near the area of the strong electric field localization. Thus, silicon surface oxidation is likely to be the origin of the rings. The oxide growth requires a supply of OH$^-$ ions. Therefore, the oxide is formed primarily inside the water meniscus due to water reduction producing OH$^-$ ions. The second oxide ring is always observed above the breakdown. By measuring the size of the oxidized area, we estimated that the meniscus size increases more than the order of magnitude for the voltage change from -20 up to -50 V. These measurements were averaged over several hundreds of dots produced with AFM-assisted nanolithography.

Two chemical reactions are responsible for oxide formation during AFM-assisted lithography. Below the breakdown, electrons migrate from the Fermi level of the electrically biased AFM tip into the water meniscus thus electrochemically reducing the water at the tip–surface interface and yielding hydroxyl ions (OH$^-$) and H$^{\cdot}$ radicals as follows: H$_2$O + e$^- \rightarrow$ H$^{\cdot}$ + OH$^-$. The hydroxyl ions are electrostatically attracted to the silicon surface, and produce an oxide. The H$^{\cdot}$ radicals may recombine and form
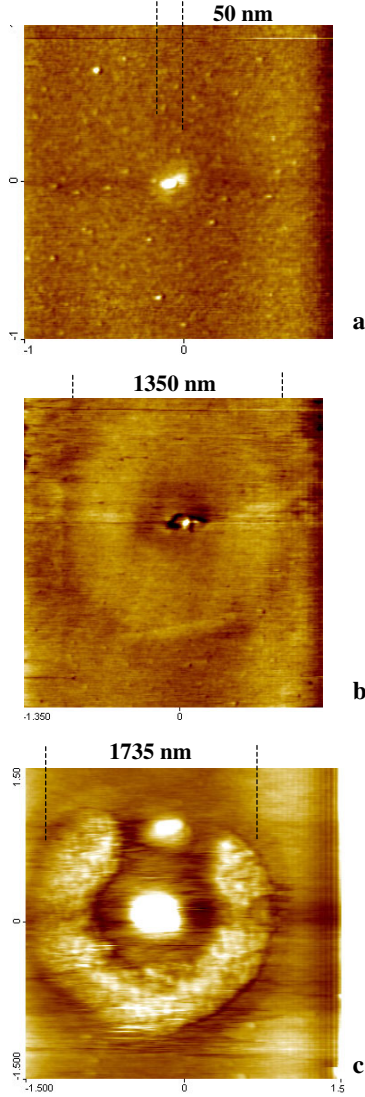
50 nm

a

1350 nm

b

1735 nm

c

Figure 4. AFM contact mode images of the oxide structures produced on the n-silicon surface (a) $V = -5$ V, $i < 0.1$ nA, below the breakdown; (b) $V = 20$ V, $i = 250$ μA, breakdown; (c) $V = -45$ V, $i = 400$ μA, above the breakdown. The formation of an additional ring is associated with oxide growth in the areas of maximal hole density.

molecular hydrogen (H$_2$) escaping from the reaction area. The electrochemical reaction near the AFM tip may be presented as $2H_2O + 2e^- \rightarrow H_2\uparrow + 2OH^-$. This electrochemical process reaches saturation when the electric field is close to the breakdown ($E = 10^8$–10^9 V m^{-1}) because the anodic process is limited due to the space charge accumulation at the interface. Thus, an electric current during this reaction has a Faradaic character with conduction provided mainly by the migration of OH$^-$ ions. The reaction at the silicon surface can be written as $Si + 2OH^- - 4e^- \rightarrow SiO_2 + 2H^+$. The net electrochemical reaction resulting in silicon oxidation is $Si + 2H_2O \rightarrow SiO_2 + 2H_2\uparrow$. The i–V dependence of this current has a nearly exponential behaviour (figure 1(a)).

The voltage increase results in breakdown including field-induced ionization of the water molecules yielding electrons, protons and free radicals (OH$\cdot$) as follows: $H_2O \rightarrow e^- + OH\cdot + H^+$. There are three options for OH$\cdot$

consumption. They may either recombine forming hydrogen peroxide H$_2$O$_2$ molecules: $OH\cdot + OH\cdot = H_2O_2$, couple with H$\cdot$ radicals producing water: $OH\cdot + H\cdot = H_2O$, or could be electrochemically reduced to hydroxyl ions at the tip–surface interface: $e^- + OH\cdot = OH^-$. Either way there is a yield of electrons capable of migrating through the water meniscus and penetrating inside the semiconductor. The current dominated by electrons obeys a linear Ohmic dependence, observed experimentally and presented in figure 1(b).

A space charge layer at the water–silicon interface consists of an ionic layer of hydroxyl ions concentrated near the interface in water, and an 'electronic' inverted layer of holes in the semiconductor due to the bending of energy bands. The ionic layer consists of a monolayer of immobile hydroxyl ions, which is normally 3–5 Å deep for hydrated ions and a diffusive layer of mobile ions at thickness comparable with the Debye screening length of ions in water given by $L_D = \sqrt{\frac{\varepsilon\varepsilon_0 RT}{2e^2 N_A^2 c_i^0}}$ [14], where ε is the dielectric constant of the electrolyte, ε_0 is permittivity of free space, R is the gas constant, $T = 293$ K is the temperature, e is electron charge, N_A is Avogadro's number, and c_i^0 is the mole concentration of the ions effectively creating the space charge. The mole concentration is given by $c_i^0 = \frac{n_i^0}{N_A}$, where the surface charge concentration is $n_i^0 = 5 \times 10^{26}$ m^{-3} [15]. The choice of ε depends on the degree of polarization of the water molecules. In a strong electric field $\varepsilon = 7$, while the normal value is 81. This gives the range for the Debye screening length 1–3.4 Å, and for the total length of the ionic part of the space charge layer 4–8.4 Å.

The depth of the 'electronic' part of the layer inside the semiconductor again is proportional to the Debye screening length and associated with the hole concentration in silicon near the water-semiconductor interface $L_D = \sqrt{\frac{\varepsilon_{Si}\varepsilon_0 k_B T}{e^2(n_e+n_h)}}$ [16], where $\varepsilon_{Si} = 12$ is the dielectric permittivity of silicon, k_B is Boltzman's constant, n_e and n_h are the concentrations of electrons and holes in silicon, respectively. For n-type silicon we may neglect hole density, and selecting $n_e \cong 4 \times 10^{19}$ m^{-3} corresponding to resistivity of 115 Ω cm^{-1}, we end up with $L_D = 650$ nm at room temperature. Thus the depth of 'electronic' part of space charge layer is much longer that that for the ionic one.

A schematic representation of the tip–silicon interface is shown in figure 5. The anomalous current is associated with the breakdown in the part of the space charge layer inside the water meniscus near the semiconductor surface and inside the semiconductor in which a large number of electron–hole pairs is generated. An avalanche breakdown occurs both in the water meniscus and in the part of the space charge region inside the semiconductor. This suggests that the threshold voltage should depend on the doping level since it affects space charge layer parameters. We observe this trend experimentally for differently doped n-type silicon samples with growths of threshold voltage for higher doping concentrations.

The Ohmic character of the electric current, and multiple observations of the rings around the oxide dots formed for the bias voltages exceeding the threshold voltage both indicate electron-type conductivity during the breakdown conditions. The hydrated electrons produced in the volume of the ionized water meniscus move through the space charge layer consisting of the OH$^-$ ions and holes in the vicinity of the interface.
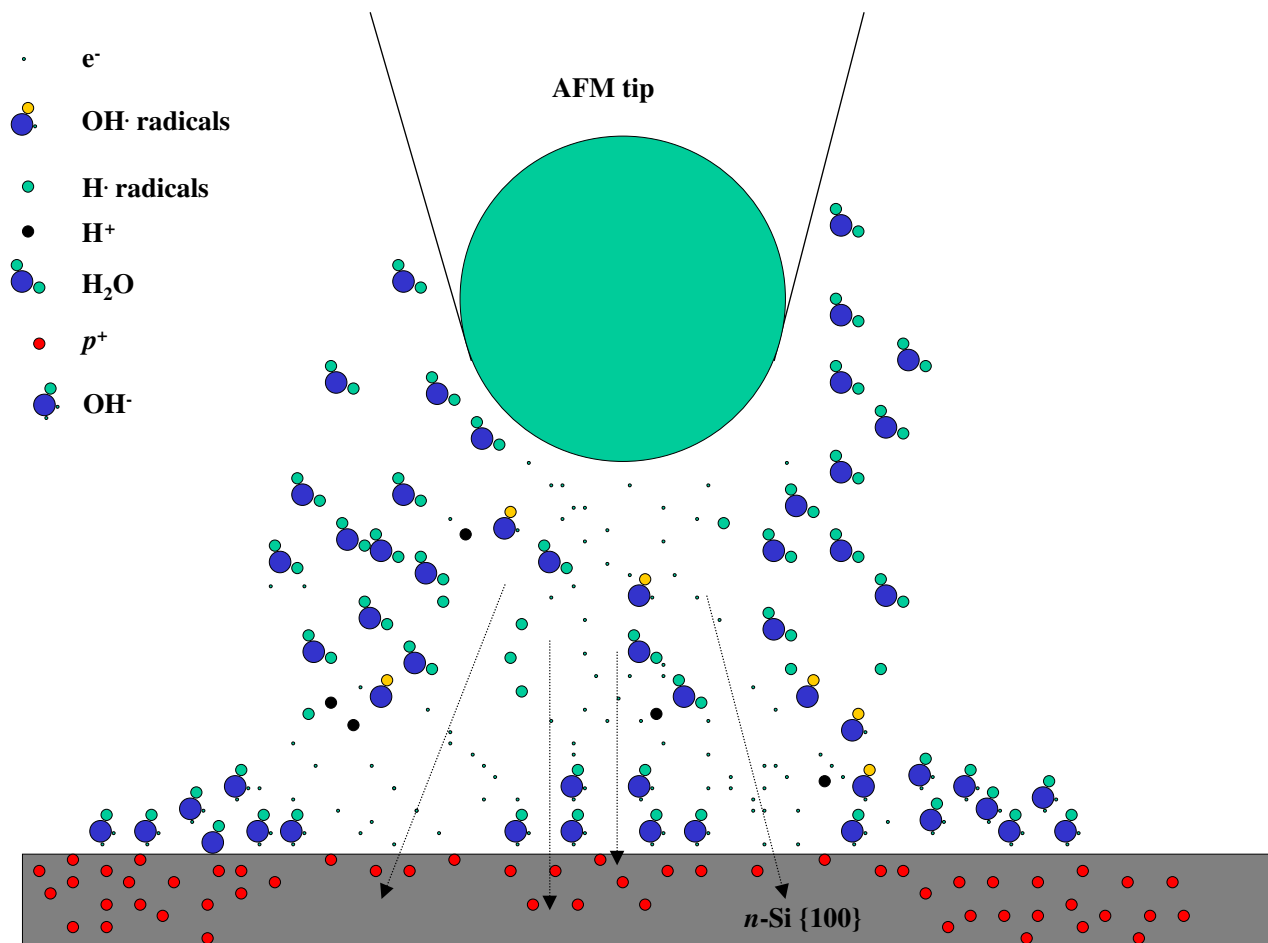
Figure 5. Schematic representation of an AFM tip–surface junction during AFM-assisted oxidation. The anomalous current is associated with an avalanche breakdown in the part of the space-charge layer inside the water meniscus and also inside the semiconductor in which a large number of electron–hole pairs is generated. Competition between recombination of electrons and holes, and the variation of field-induced hole concentration results in regions of depleted holes. OH$^-$ ion distribution follows the distribution of the hole concentration, which leads to oxide growth in the areas where the concentration is maximal, and therefore in the formation of oxide rings.

They recombine with the holes producing electronic current. A possible explanation for the ring formation could be the following. The effective density of the field-induced holes near the interface increases as the normal component of the electric field increases. The density of electrons inside the meniscus is proportional to the normal component of the electric field, which falls off with the distance from the tip apex. Competition between the recombination of electrons and holes, and the variation in the field-induced hole concentration results in regions of depleted holes and affecting the formation of the space charge layer. Hydroxyl ion distribution follows the distribution of the hole concentration, which leads to the oxide growth in the areas where the concentration is maximal.

Two facts support the existence of water around an AFM tip during the breakdown. First is the continuous oxide growth at voltages above the breakdown threshold. The supply of the OH$^-$ ions producing the oxide may be related to the electrochemical reduction of water and the reduction of OH· radicals with electrons produced as a result of the water ionization. Second, is the comparative growth of the snap-off force with respect to the snap-on force in all the recorded force–distance curves indicating the existence of the capillary tip–surface interaction. We also considered the

possibility of plasma ball formation during the breakdown. It is well known that a plasma ball must be electrically neutral within the confinement region meaning that the Debye screening length must be small with respect to the diameter of the region. An estimate for the minimum screening length of 'cold' plasma is 2 μm, assuming that $kT_e = 1$ eV, and the electron concentration is $n_e = 10^{-18}$ m^{-3}. The tip–sample separation is about several hundred nanometres even for the maximum voltage we used (-50 V) during the breakdown. So a plasma ball must occupy a much larger region to be stable between the tip and the surface, and therefore, we exclude the possibility of plasma ball formation during the breakdown. The existence of water in the tip–surface junction, and the field-induced ionization of water molecules resulting in hydrated electrons, plays an important role in creating conductive channels that allow electrons to travel from the Fermi level of the tip to the conduction zone of silicon.

Nanolithography is at the heart of contemporary nanotechnology, or the 'top–down' approach as introduced by Feynman [17]. Two main disadvantages of AFM-assisted lithography are the lack of speed, and the limit imposed on the nanostructure's size (10–20 nm) related to the AFM tip

radius. This is a serial process, in that each line or dot is written individually and sequentially. The linear speed of the AFM-assisted lithography is 10–10^3 μm s^{-1}, which is slow even with highly sensitive resist. The observation of a strong electronic current suggests making the process parallel. A large water meniscus diameter (more than several hundred of nanometres) during breakdown, the high density of the electric current (and therefore fast transport of charge within short time intervals), as well as electron-type conductivity may allow electrons to interfere constructively should the following three conditions be satisfied:

(1) the mean free path of the electrons is comparable or larger than the tip–surface distance;
(2) two or more identical electron beams must be generated;
(3) the beams must have the same temporal and spatial coherence.

Two identical electron beams inside the water meniscus could be produced via the shape of the AFM tip. An AFM tip can be milled into a fork-like shape, consisting of two identical tips, with a focused ion beam down to nanometre size. This may provide the necessary separation between two tips to assist the electron holography principle. Nanoscale electron holography requires additional theoretical considerations, and is the subject of experimental verification, which is out of the range of this paper.

We have observed an anomalously high current during AFM-assisted lithography on the surface of n-type silicon resulting in symmetrical rings forming around the original oxide spot. This current obeys Ohmic i–V dependence related to an electronic type of conductance, which is different to the ionic current used in conventional AFM-assisted nanolithography on silicon. Double space charge layer formation on the water–silicon interface is considered in detail. Electronic-type conductivity suggests that the electrical breakdown occurs inside the water meniscus and the space charge layer near the silicon surface. The existence of water in the tip–sample junction during the breakdown and its field ionization are important factors enabling the formation of the conductance channels connecting the tip and the sample. We have studied this breakdown current up to −50 V applied to an AFM tip and observed that the current can be sustained for a few minutes after voltage application. The stability of this anomalous current may be useful for nanoscalar charge transport, and opens up new opportunities for AFM-assisted nanolithography.

Acknowledgments

References

[1] Binning G, Quate C F and Gerber Ch 1986 *Phys. Rev. Lett.* **56** 930
[2] Dagata J A, Schneir J, Harary H H, Evans C J, Postek M T and Bennet J 1990 *Appl. Phys. Lett.* **56** 2001
[3] Snow E S, Campbell P M and McMarr P J 1993 *Appl. Phys. Lett.* **63** 749
[4] Perez-Murano F, Abadal A, Barniol N, Aymerich X, Servant J, Gorostiza P and Sanz F 1995 *J. Appl. Phys.* **78** 6797
[5] Legrand B and Stievenard D 1999 *Appl. Phys. Lett.* **74** 4049
[6] Perez-Murano F, Birkelund K, Morimoto K and Dagata J A 1999 *Appl. Phys. Lett.* **75** 199
[7] Campbell P M, Snow E S and McMarr P J 1995 *Appl. Phys. Lett.* **66** 1388
[8] Minnie S C, Soh H, Flueckiger P and Quate C F 1995 *Appl. Phys. Lett.* **66** 703
[9] Matsumoto K, Ishii M and Segawa K 1996 *J. Vac. Sci. Technol.* B **14** 1331
[10] Cohn R W, Lyuksyutov S F, Walsh K M and Crain M M 1999 *Opt. Rev.* **6** 345
[11] Snow E S, Park D and Campbell P M 1996 *Appl. Phys. Lett.* **69** 269
[12] Avouris Ph, Martel R, Hertel T and Sandstorm R 1998 *Appl. Phys.* A **66** S659
see also
Avouris Ph, Hertel T and Matrel R 1997 *Appl. Phys. Lett.* **71** 285
[13] Bloess H, Staikov G and Schultze J W 2001 *Electrochim. Acta* **47** 335
[14] McHardy J and Ludwig F (ed) 1992 *Electrochemistry of Semiconductors and Electronics: Processes and Devices* (Park Ridge, NJ: Noyes)
[15] Dagata J A, Inome T, Itoh J and Yokoyama H 1998 *Appl. Phys. Lett.* **73** 271
[16] Morrison S R 1980 *Electrochemistry at Semiconductor and Oxidized Metal Electrodes* (New York: Plenum)
[17] Feynman R 1959 There is a plenty room at the bottom, APS Talk, Pasadena, CA